

# Cavity nonlinear optics with few photons and ultracold quantum particles

András Vukics,\* Wolfgang Niedenzu, and Helmut Ritsch

*Institute for Theoretical Physics, University of Innsbruck, Technikerstr. 25, A-6020 Innsbruck, Austria*

The light force on particles trapped in the field of a high- $Q$  cavity mode depends on the quantum state of field and particle. Different photon numbers generate different optical potentials and different motional states induce different field evolution. Even for weak saturation and linear polarizability the induced particle motion leads to nonlinear field dynamics. We derive a corresponding effective field Hamiltonian containing all the powers of the photon number operator, which predicts nonlinear phase shifts and squeezing even at the few-photon level. Wave-function simulations of the full particle-field dynamics confirm this and show significant particle-field entanglement in addition.

It is commonly assumed that offresonant interaction of coherent light with a linear polarizable medium only creates linear phase shifts and coherent states of the scattered light. This is especially the case for weak light fields involving only few photons, where generating any nonlinear phase shift is a serious challenge [1] while such devices would be highly desirable in photonics or quantum information applications [2]. One possibility to generate nonlinear phase shifts even at the single photon level was demonstrated via resonant strong coupling of an atomic transition and a photon in a high- $Q$  cavity [3]. Recently it was noted that nonclassical light fields can also emerge from linear scattering off a weakly excited medium, if its motional state has genuine quantum properties [4]. Here we combine those two ideas and study the effective nonlinear cavity field dynamics generated from the photon number dependence of light forces on the quantum particle motion in the cavity-enhanced optical potential [5].

In a prototype setup an ultracold particle is placed in the optical potential generated by a cavity field mode. For large detuning between atomic and cavity resonance spontaneous emission is small and the cavity field simply generates a photon-number dependent trapping potential. For any superposition state involving several photon numbers, as e.g. a coherent state, the localization of the particle thus differs for each photon number. As the particle position spread in turn determines effective refractive index and field phase shift this implies effective nonlinear field evolution. Experimentally a closely related nonlinear effect was found in a pioneering setup in Berkeley [6]. As several similar setups coupling a BEC to a high- $Q$  cavity mode have just been realized [7], further detailed experimental studies will emerge soon.

Naturally the coupled particle-field dynamics generates entanglement, which partly persists even in a steady state, where each photon number is correlated with a different particle state. Interestingly, even after tracing over the particle degrees of freedom the field exhibits nonclassical properties and its dynamics can be approximated by a simple effective field Hamiltonian. We study its central predictions, and check its validity by a full particle-field

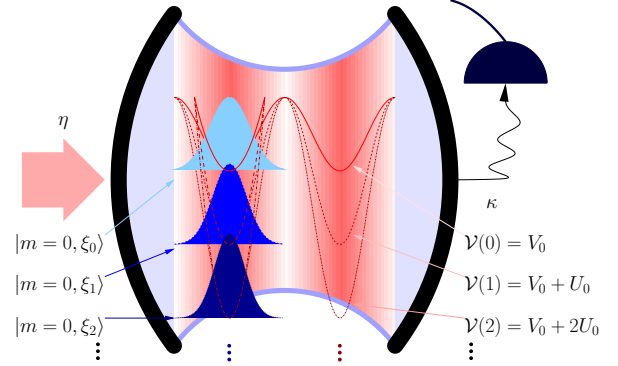


FIG. 1: (Color online) Scheme of the system with a quantum particle in the field of a driven cavity. A single driven standing wave mode generates optical potentials of different depth depending on the photon number. We also display the corresponding particle ground-state wavefunctions.

wave-function simulation.

Our prototype CQED system is depicted in Fig. 1. Following standard assumptions for a particle moving in 1D along the axis of a far red detuned single cavity mode, we start from a Jaynes-Cummings Hamiltonian with eliminated internal state(s) [8, 9] to get ( $\hbar = 1$ ):

$$H = \frac{p^2}{2\mu} + (V_0 + U_0 a^\dagger a) f(Kx) - \Delta_C a^\dagger a + i\eta (a^\dagger - a). \quad (1)$$

Here  $x$ ,  $p$ , and  $\mu$  are the particle position and momentum operators and its mass;  $a$  is the field operator,  $K$  is the mode wave number,  $\Delta_C = \omega - \omega_C$  is the cavity detuning ( $\omega$  is the laser,  $\omega_C$  is the mode frequency),  $\eta$  is cavity pump amplitude.  $V_0$  describes an additional c-number potential along the cavity axis, it ensures a particle bound state in the absence of cavity photons, but can be neglected for larger photon numbers. A central parameter here is  $U_0$ , the optical potential depth per photon, which also gives the cavity frequency shift per particle and is proportional to the particle susceptibility [9]. As we consider small cavities, photon loss is important even for good mirrors and will be described by the standard Liouvillean [10]  $\mathcal{L}\rho = \kappa (2a\rho a^\dagger - [a^\dagger a, \rho]_+)$ , where  $\kappa$  is the mode linewidth. In the following  $\mathfrak{M}(H)$  stands for a *Master equation* defined by Hamiltonian  $H$

\*Electronic address: andras.vukics@uibk.ac.at

and this Liouvillean.

The most interesting part of the dynamics arises from the second term of the Hamiltonian (1) describing dispersive particle-field interaction. Its effect can clearly be seen from an expansion of the wavefunction in a product basis  $|\Psi\rangle = \sum_n \Psi_n |n\rangle |\phi_n\rangle$ , where  $|n\rangle$  is the  $n$ -photon field state and  $|\phi_n\rangle$  a particle wavefunction, which will evolve subject to the potential  $\mathcal{V}(n) f(Kx)$  [16]. Naturally, this creates entanglement between the particle and field on the timescale of the particle motion, characterized by  $\omega_{\text{rec}}$ . The pump term proportional to  $\eta$  in the Hamiltonian (1) and the photon loss described by quantum jumps (application of operator  $a$  on the state vector) on the other hand mix the different evolution branches and thus tend to reduce the entanglement.

The fullness of this very intricate stochastic dynamics can be captured only by a simulation performed on the product basis of the mode-particle Hilbert space, which leads to high dimensionality even for a single particle [11, 12]. Fortunately to understand the central physics, such a brute force approach is not necessary and we will present a systematic method for identifying a much lower dimensional but sufficient subspace in this immense Hilbert space. It is spanned by separable particle-field states, which represent the full quantum trajectories very well after an initial transitional period. The idea should be generally applicable in situations where two quantum mechanical systems interact and one of them is dissipative — a situation ubiquitous in cavity QED, but also e.g. in a multi-level atom where the dissipative internal degree of freedom and the motion are coupled by a spatially dependent pump.

As the cavity field is well represented by a standing wave cosine mode with wave number  $K$ ,  $f(Kx) = \cos^2(Kx)$ , the Hamiltonian commutes with the parity operator so that the dynamics does not mix the symmetric and antisymmetric subspaces of the particle Hilbert space and we will restrict ourselves to the symmetric part only. To further simplify the mathematics in the following we add a sufficiently strong classical part to the cosine potential, so that with  $V_0, U_0 < 0$  we are allowed a harmonic approximation  $f(Kx) \approx 1 - (Kx)^2$ . At the same time we redefine the detuning  $\Delta_C - U_0 \rightarrow \Delta_C$  and  $\mathcal{V}(X) \equiv |V_0| + |U_0| X$ .

Let us now construct a subspace spanned by separable states, which works well in the regime of moderate coupling in the sense that the expectation value of the projector to the subspace is close to unity for most of the time on a trajectory. As a particle with a *fixed* state vector cannot get entangled with the field, we get a coherent steady state in the mode. Therefore, if we fix the particle in a harmonic oscillator eigenstate, the corresponding stationary field is a coherent state  $|\alpha\rangle$ , which can be simply calculated as the particle merely causes a frequency shift of the mode by  $|U_0| K^2 \langle x^2 \rangle$ . This coherent state in the mode creates an additional average potential for the particle reading  $\mathcal{V}(|\alpha|^2) (Kx)^2$ . For the combined potential we then can again calculate the corresponding

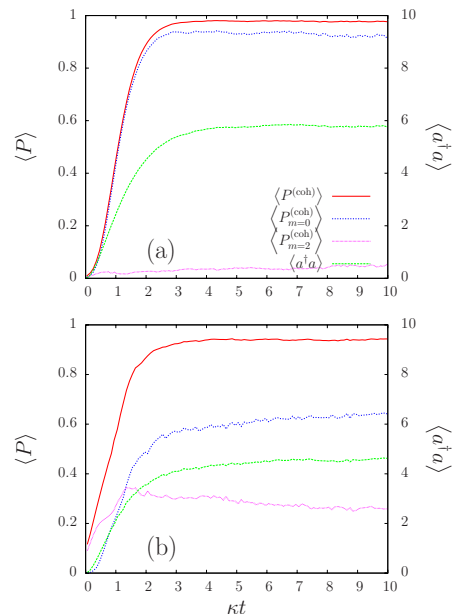


FIG. 2: (Color online) System time evolution using an ensemble of 300 trajectories started from a product state of vacuum for the mode and (a)  $|0, \xi_0\rangle$ , (b)  $(|0, \xi_0\rangle + |2, \xi_0\rangle)/\sqrt{2}$ . After a transitional period during which the photon number grows from 0 to its quasi steady-state value the system arrives into the subspace  $\mathcal{E}^{(\text{coh})}$ , where it stays from then on, so that  $\langle P^{(\text{coh})} \rangle$  is close to one. Parameters:  $(\kappa, V_0) = (10, -100)\omega_{\text{rec}}$ ,  $(\Delta_C, \eta, U_0) = (0, 2.5, -10)\kappa$ . This  $U_0$  value represents a moderate coupling regime for our purposes.  $P_{0,2}^{(\text{coh})}$  represent the projectors to only the states corresponding to  $m = 0, 2$ . As we see, the population in these two states in the quasi steady-state differs from that in the initial condition (50–50%): the  $m = 0$  state has higher population, in which the cavity cooling effect [13] is manifested at work.

particle eigenstate. Iterating this process (or simply solving a corresponding nonlinear equation for  $\alpha$ ) we find the subspace

$$\mathcal{E}^{(\text{coh})} \equiv \text{span} \left\{ |\alpha_m\rangle \left| m, \xi_{|\alpha_m|^2} \right\rangle \right\}_{m \in \mathbb{N}},$$

where the particle state is a harmonic oscillator eigenstate with oscillator length  $\xi_{|\alpha_m|^2}$  determined together with  $\alpha_m$  self consistently.

In Fig. 2 we demonstrate that  $\mathcal{E}^{(\text{coh})}$  is a very suitable subspace to represent the full coupled particle-field dynamics in the moderate coupling regime. This is done by calculating the expectation value of the subspace's projector  $P$  for a state obtained from Monte Carlo wavefunction simulations of the full coupled dynamics with a dimension of  $\approx 2000$  [12].

Being based on self-consistent product states, the above method for obtaining  $\mathcal{E}^{(\text{coh})}$  contains essential parts of the nonlinear field dynamics but completely disregards the expected particle-field entanglement. Hence this ansatz (and the subspace  $\mathcal{E}^{(\text{coh})}$ ) is unsuitable for stronger coupling where we have to use an extended

approach involving a somewhat larger set of separable states. While the particle states will still be harmonic-oscillator eigenstates in self-consistent average potentials, the corresponding mode states have to be determined by a new Master equation based on an effective nonlinear Hamiltonian invoking all the powers of the photon number operator. Note that although it is eliminated from the dynamics it is the very *quantum nature* of the motion of the *linearly polarizable* particle, which creates this nonlinearity. Besides giving a very good intuition to the underlying dynamics, it is a significant boon of this approach that we are left with a dynamics to be solved solely on the mode Hilbert space, with a much smaller dimension. We start the derivation by casting the Hamiltonian (1) into the form

$$H_{\text{HO}} = \Omega (a^\dagger a) \left( b^\dagger b + \frac{1}{2} \right) - \Delta_C a^\dagger a + i\eta (a^\dagger - a). \quad (2)$$

The first two terms of that Hamiltonian in the harmonic-oscillator approximation can be conveniently expressed using the ladder operator defined as  $b \equiv (\xi_{a^\dagger a}^{-1} \otimes x + i\xi_{a^\dagger a} \otimes p)/\sqrt{2}$ , so that it is an operator on the complete mode-particle Hilbert space. Note for future reference that  $b, b^\dagger$  still obey the usual commutation relations. Recall that the frequency  $\Omega(a^\dagger a)$  is an operator on the mode Hilbert space.

Consider now the following basis:  $|n, m\rangle \equiv |n\rangle |m, \xi_n\rangle$ , where  $|n\rangle$  is the  $n$ th Fock state of the mode, while  $|m, \xi_n\rangle$  is again the  $m$ th harmonic oscillator eigenstate corresponding to the oscillator length determined by the state of the mode (c.f. also Fig. 1). Due to this dependence the basis is *not* a direct product of bases in the subsystems' Hilbert spaces. Nevertheless, it is an orthogonal basis, since the Fock states for different  $n$  are orthogonal, while for a given  $n$  the  $|m, \xi_n\rangle$  states are orthogonal for different  $m$  since they have the same oscillator length. We now partition the Hilbert space to subspaces with a given  $m$   $\mathcal{E}_m \equiv \{|n, m\rangle\}_{n \in \mathbb{N}}$  with projectors  $P_m \equiv \sum_n |n, m\rangle \langle n, m|$ .

Let us project the Master equation  $\mathfrak{M}(H_{\text{HO}})$  to the subspace  $\mathcal{E}_m$ . It is an invariant subspace of the first ( $H^{(\text{int})}$ ) and second terms of the Hamiltonian (in fact, the  $|n, m\rangle$  states are eigenstates), so that e.g.  $H^{(\text{int})} = \sum_m P_m H^{(\text{int})} P_m$ . This is not true, however, for the pump term (third term of the Hamiltonian (2)) and the Liouvillian, since operator  $a$  mixes the subspaces with different  $m$ . Indeed,  $a|n, m\rangle \propto |n-1\rangle |m, \xi_n\rangle$ , and  $\langle m', \xi_{n-1} | m, \xi_n\rangle \neq 0$  for all  $m'$ , therefore  $\langle n-1, m' | a | n, m\rangle \neq 0$ . In a first approximation we neglect the coupling between the  $\mathcal{E}_m$  subspaces by the operator  $a$  and assume  $H \approx \sum_m P_m H P_m$  for the complete Hamiltonian (2) and the Liouvillian. A mathematical justification of this is that  $\xi_n$  is only slowly varying with  $n$ , so that the corresponding eigenfunctions are almost orthogonal. All approximations are *a posteriori* confirmed by numerical tests. Within this approximation the dynamics can be solved separately in the different  $\mathcal{E}_m$  subspaces. Note that the projected field operator is

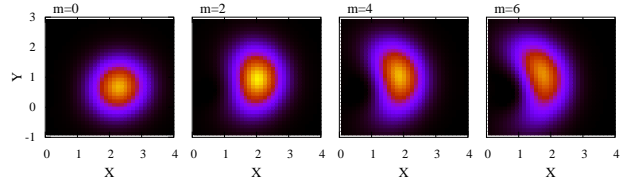


FIG. 3: (Color online) Wigner functions calculated from the stationary field density matrix  $\rho_{m;n,n'}^{(\text{ss})}$  for different vibrational particle states  $m$ . Same parameters as for Fig. 2, but  $\Delta_C$  is always adjusted to resonance, i.e. in the Hamiltonian (3) the term linear in  $a^\dagger a$  vanish. While for  $m=0$  the state is almost coherent the Wigner function becomes more and more banana-shaped with increasing  $m$ .

approximated  $P_m a P_m \approx \sum_m \sqrt{n+1} |n, m\rangle \langle n+1, m|$ , and that this approximation is not crucial, but it yields that the usual  $a$  operator will appear in the projected Master equation  $\mathfrak{M}(H_m)$ . Within this framework we can find the steady-state density operator in the subspace  $\mathcal{E}_m$ , which has the dimension of only the field Hilbert space, of the form  $\rho_m^{(\text{ss})} \equiv \sum_{n,n'} \rho_{m;n,n'}^{(\text{ss})} |n, m\rangle \langle n', m|$ , where  $\rho_{m;n,n'}^{(\text{ss})}$  is *formally* a density matrix only on the mode Hilbert space. It is the steady-state solution of  $\mathfrak{M}(H_m)$  with effective Hamiltonian

$$H_m \equiv \sqrt{\omega_{\text{rec}} (|V_0| + |U_0| a^\dagger a)} (2m+1) - \Delta_C a^\dagger a + i\eta (a^\dagger - a). \quad (3)$$

Note that for  $\omega_{\text{rec}} = 0$  we recover the standard single mode Hamiltonian linear in  $a^\dagger a$ , which yields pure coherent states in steady state.

From a Hamiltonian (1) linear in  $a^\dagger a$ , but containing the particle-mode interaction, we have hence arrived at the conditional Hamiltonian (3) nonlinear in  $a^\dagger a$  operating only on the field Hilbert space. In Fig. 3 we illustrate the nonclassical states this Hamiltonian generates. As striking example one obtains banana-shaped Wigner functions for higher  $m$  indices.

To find a subspace which represents  $\rho_m^{(\text{ss})}$  well, we adopt an idea from the density matrix renormalization group method [14]. We diagonalize the density operator and take a (usually small) number of eigenvectors corresponding to the leading eigenvalues — in fact, we introduce a cutoff at a given value  $\epsilon \ll 1$  in the spectrum. Let us remark here that for parameters we studied in practice,  $\rho_m^{(\text{ss})}$  was always very close to a pure state (largest eigenvalue very close to unity). We obtain the states  $|\Psi_{m,i}\rangle \equiv \sum_n \Psi_{m,i;n} |n, m\rangle$ , where  $i$  indexes the different eigenvectors. It runs between 1 and  $N_m$ , which latter is a number depending on  $\epsilon$  and it may be different for different  $m$  indices.

Our most salient approximation is that at this point we approximate these states by separable states:

$$|\Psi_{m,i}\rangle \approx |\phi_{m,i}\rangle |m, \xi_{\langle \phi_{m,i} | a^\dagger a | \phi_{m,i} \rangle}\rangle \equiv |e_{m,i}\rangle, \quad (4)$$

with  $|\phi_{m,i}\rangle \equiv \sum_n \Psi_{m,i;n} |n\rangle$ .

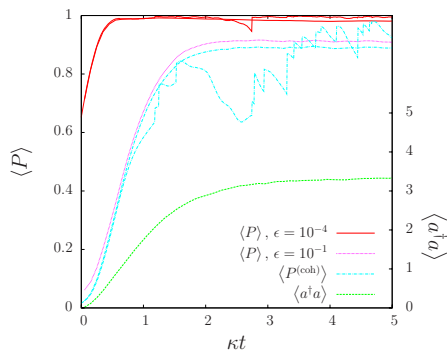


FIG. 4: (Color online) Projector expectation values in the strong coupling regime  $(\Delta_C, \eta, U_0) = (0, 2.5, -100)\kappa$ . Ensemble of 300 trajectories. With  $\epsilon = 10^{-1}$   $N_m = 1$  for all  $m$ , while with  $\epsilon = 10^{-4}$   $N_0 = 3$ ,  $N_2 = 2$ ,  $N_{m>2} = 1$ . In both cases  $\langle P \rangle > \langle P^{(\text{coh})} \rangle$ , but indeed in the second case  $\langle P \rangle \approx 1$  after a transitional period. In thin lines results from a typical *individual* trajectory are displayed to show that the quality of  $\mathcal{E}^{(\text{coh})}$  fluctuates wildly on a single trajectory, while that of  $\mathcal{E}$  remains close to unity even in this case.

Note that the particle state has been taken to be an  $m$ th harmonic oscillator eigenstate corresponding to the oscillator length calculated from the average photon number of the mode state  $|\phi_{m,i}\rangle$ . This approximation is on one hand again justified by the aforementioned mathematical argument, but also by a physical argument: during the dynamics the pump term and the quantum jumps mix the levels of different  $n$ , and a particle with finite mass cannot follow this mixing immediately. In addition it is *a posteriori* justified by simulations. For the sake of further intriguing the reader we note that the states  $|e_{m,i}\rangle$  are not even in the subspace  $\mathcal{E}_m$  to which we projected our Master equation in the first place.

We readily arrive at the subspace

$$\mathcal{E} \equiv \text{span} \{ |e_{m,i}\rangle \}_{m \in \mathbb{N}, i=1 \dots N_m}$$

spanned by separable states, for which the mode states are leading eigenvectors of a density matrix, which is a steady-state solution of  $\mathfrak{M}(H_m)$  containing the square root of  $\mathcal{V}(a^\dagger a)$  and hence all the powers of the photon number operator. In Fig. 4 we demonstrate that this is a very high quality subspace even in the (for our purposes strong coupling) regime where the formerly derived subspace  $\mathcal{E}^{(\text{coh})}$  breaks down. As expected, the quality of  $\mathcal{E}$  can be increased by decreasing the cutoff parameter  $\epsilon$ .

In Fig. 5 we demonstrate one more experimentally very easily accessible situation, which clearly exhibits the non-classicality of the field generated by particle-field entanglement. Here to even more distill the central physical effect, the cavity is chosen to be unpumped, but a few-photon coherent state is prepared in the mode, which

then slowly leaks out. The particle is started from the ground state wave packet of the complete potential, so that the system is initially in a product state. Note that via the generated entanglement the particle is capable to

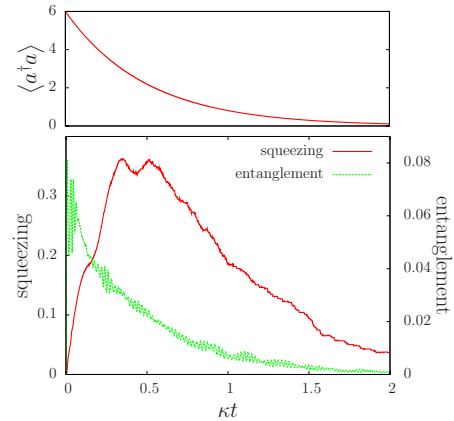


FIG. 5: (Color online) Time evolution (300 trajectories) from an initial product state. Parameters:  $(\kappa, V_0) = (0.1, -60)\omega_{\text{rec}}$ ,  $(\Delta_C, \eta, U_0) = (0, 0, -100)\kappa$  — the particle is chosen to be very light in comparison to previous cases, so that it can be influenced more easily by the field. The arising field squeezing is measured by  $-\log(\lambda_s)$ , where  $\lambda_s$  is the smaller eigenvalue of the field quadratures' correlation matrix. The particle-field entanglement is measured by the negativity of the density operator's partial transpose [11, 15].

transform the initial coherent field state into a squeezed state.

We demonstrated that few photon nonlinear optics can be implemented even by help of a linearly polarizable medium, if one includes spatial dynamics of the medium. In the low temperature limit where the medium has genuine quantum properties, a coherent state input field then can get entangled with the motional states. Surprisingly this complex coupled dynamics can be described by an effective nonlinear field Hamiltonian which can be tailored to experimental needs. As it operates only on a restricted Hilbert space it can be efficiently simulated. In our example we could identify an  $O(10)$  dimensional subspace of the complete  $O(1000)$  dimensional Hilbert space to which the system dynamics was confined with high probability. While we have concentrated on a single quantum particle here, an analogous dynamics will emerge in the many particle case if one invokes only the lowest few collective excitations of the ensemble. This case will also show a strongly increased nonlinearity via collective enhancement and open the route to nonlinear optics with single photons.

**Acknowledgments:** work supported by Austrian Science Fund projects P17709+I119 N16

- 
- [1] Y. R. Shen, Phys. Rev. **155**, 921 (1967).
- [2] A. Imamoglu, H. Schmidt, G. Woods, and M. Deutsch, Phys. Rev. Lett. **79**, 1467 (1997).
- [3] Q. A. Turchette, C. J. Hood, W. Lange, H. Mabuchi, and H. J. Kimble, Phys. Rev. Lett. **75**, 4710 (1995).
- [4] I. B. Mekhov, C. Maschler, and H. Ritsch, Nature Physics **3**, 319 (2007). I. B. Mekhov, C. Maschler, and H. Ritsch, Phys. Rev. Lett. **98**, 100402 (2007).
- [5] M. Gangl and H. Ritsch, Phys. Rev. A **61**, 011402 (1999). C. Maschler and H. Ritsch, Phys. Rev. Lett. **95**, 260401 (2005).
- [6] S. Gupta, K. L. Moore, K. W. Murch, and D. M. Stamper-Kurn, Phys. Rev. Lett. **99**, 213601 (2007).
- [7] F. Brennecke, T. Donner, S. Ritter, T. Bourdel, M. Köhl, and T. Esslinger, Nature **450**, 268 (2007). Y. Colombe, T. Steinmetz, G. Dubois, F. Linke, D. Hunger, and J. Reichel, Nature **450**, 272 (2007).
- [8] P. Domokos and H. Ritsch, J. Opt. Soc. Am. B **20**, 1098 (2003).
- [9] A. Vukics and P. Domokos, Phys. Rev. A **72**, 031401 (2005).
- [10] C. W. Gardiner and P. Zoller, *Quantum Noise* (Springer, 2000).
- [11] A. Vukics, J. Janszky, and P. Domokos, J. Phys. B: At. Mol. Opt. Phys. **38**, 1453 (2005).
- [12] A. Vukics and H. Ritsch, Eur. Phys. J. D **44**, 585 (2007).
- [13] P. Horak, G. Hechenblaikner, K. M. Gheri, H. Stecher, and H. Ritsch, Phys. Rev. Lett. **79**, 4974 (1997). P. Maunz, T. Puppe, I. Schuster, N. Syassen, P. W. H. Pinkse, and G. Rempe, Nature **428**, 50 (2004).
- [14] U. Schollwöck, Rev. Mod. Phys. **77**, 259 (2005).
- [15] G. Vidal and R. F. Werner, Phys. Rev. A **65**, 032314 (2002).
- [16] We define the potential strength  $\mathcal{V}(X) \equiv V_0 + U_0 X$ , and from this the oscillator frequency  $\Omega(X)^2 \equiv 4\omega_{\text{rec}}\mathcal{V}(X)$  and the characteristic length  $(K\xi_X)^4 \equiv \omega_{\text{rec}}/\mathcal{V}(X)$ . Here  $\omega_{\text{rec}} \equiv \hbar K^2/(2\mu)$  is the recoil frequency, which gives the elementary timescale of the atomic motion on a length-scale of  $K^{-1}$ .  $X$  may stand for an operator or a c-number: hence e.g.  $\mathcal{V}(a^\dagger a)$  represents a *quantum* potential strength, while  $\mathcal{V}(n)$  is the potential created by the  $n$ -photon Fock state of the mode. We also use the notation  $|m, \xi\rangle$  for the  $m$ th harmonic oscillator eigenstate corresponding to oscillator length  $\xi$ .